Walters, M. A., & Spiro, T. G. (1983) *Inorg. Chem.* (in press).
Woodruff, W. H., Norton, K. A., Swanson, B. I., & Fry, H. A. (1983a) *J. Am. Chem. Soc. 105*, 657.
Woodruff, W. H., Norton, K. A., Swanson, B. I., & Fry, H. A. (1983b) *Proc. Natl. Acad. Sci. U.S.A.* (in press).
Woodruff, W. H., Norton, K. A., Swanson, B. I., Fry, H. A., & Malmström, B. G. (1983c) *Inorg. Chim. Acta 79*, 51.
Wright, P. G., Stein, P., Burke, J. M., & Spiro, T. G. (1979) *J. Am. Chem. Soc. 101*, 3531.
Yachandra, V. K., Hare, J., Moura, I., & Spiro, T. G. (1983) *J. Am. Chem. Soc.* (in press).
Zaslaw, B., & Rundle, R. E. (1961) *J. Phys. Chem. 57*, 490.

A Thermodynamic Model of the Lamellar to Inverse Hexagonal Phase Transition of Lipid Membrane–Water Systems†

Gregory L. Kirk, Sol M. Gruner,* and D. L. Stein

ABSTRACT: A theoretical model of the lamellar (L_α) to inverted hexagonal (H_{II}) phase transition is developed for mixtures of water and biological lipids. A free energy per lipid molecule is calculated for each phase as the sum of four lattice-specific terms: a local elastic term and global terms involving the packing of hydrocarbon chains, Debye-shielded electrostatics, and hydration effects. A critical lipid concentration for the transition is indicated by the concentration where the net lamellar and hexagonal free energies are equal. The relevance of the model to membrane interactions in biological systems is discussed. Suggestions are made for introducing temperature dependence into the model, and experiments are proposed to investigate the principal opposing forces in the model.

It is important to understand the microscopic factors governing the lamellar (L_α)[1] to inverted hexagonal (H_{II}) (Deamer et al., 1970) phase transition in biological lipids. The foremost physiological role of phospholipid is the formation of the bilayer membranes that compartmentalize cellular functions. Certain commonly encountered lipids (e.g., PE and CL) can convert to a nonbilayer phase inimical to compartmentalization, suggesting careful regulation of this transition by living cells. The L_α to H_{II} transition has been investigated experimentally by determining the phase diagrams of bulk lipid extracts vs. water concentration and temperature [see Luzzati (1968) for a review].

A major difficulty is in understanding how the experimental results on bulk systems apply to living cells. For example, it is known that bulk PE–water mixtures undergo a lamellar to H_{II} transition at physiological temperatures as the water concentration is decreased (Reiss-Husson, 1967). It is often argued that these conditions bear little relevance to living cells because cells always contain much water. This argument is misleading in that it ignores the range and nature of the microscopic forces driving the phase transition and the diversity of microenvironments encountered in cells. To illustrate, consider a comparison of the local conditions in two situations. In the first, consider the free energy of a lipid molecule in a bulk lamellar lipid–water mixture, undergoing the lamellar to H_{II} phase transition. In the second, consider the free energy of the lipid molecule in the near-contact zone between two closely opposed membrane vesicles, as in vesicle fusion. In either case, the lipid molecule in a bilayer environment faces a thin aqueous layer and is subject to the strong short-range (<50-Å) forces present between membrane surfaces.

In this paper, it is shown that the net free energy rises steeply as the thickness of the intervening aqueous space between the bilayers decreases. The free energy rises less steeply for a local cluster of inverted lipid tubes with the same succession of lipid to water ratios. At some point, the free energies cross, and it becomes energetically favorable for the lipid to be in the inverted cylinder geometry. Locally, the situation is similar in both the bulk lipid and the approaching vesicle cases. It is in this local sense that one may use the experimental data on isolated bulk systems and consider the applicability of the model to cells.

We assume that the minimum free energy of a given number of lipid and water molecules is dominated by four geometry-dependent forces: lipid monolayer elasticity (curvature), electrostatics, hydrocarbon chain packing, and a surface hydration force. Three specific geometries are considered: lamellar, H_{II}, and close-packed inverted spherical micelles. In each case, a free energy associated with each of the four interactions is computed at a given lipid to water ratio. The geometry with the lowest total free energy is taken as the energetically favored phase at that concentration. This is used to predict the sequence of the three phases that would be observed in a bulk lipid–water system in equilibrium as a function of concentration. We consider three geometries consistent with the constraints of the hydrophobic effect. Rigorously, one would have to apply the approach to all possible geometries to predict the equilibrium state. In bulk lipid systems, lamellar and H_{II} phases *do* occur; consequently, it is logical, and computationally tractable, to apply the approach to them. In cells, the boundary conditions are more complex and more geometries must be considered. The important point is that, given a pair of geometries, this approach may be used to determine which of the two is favored in equilibrium. Cellular systems are additionally complicated by the effects of other components (e.g., proteins) and nonequilibrium behavior. Because the approach specifies a well-defined local free energy, it may be used in cases where no distinct lattice exists. Examples are intermembrane particles (deKriujff et al., 1979), tight junctions (Pinto da Silva,

† From the Department of Physics, Joseph Henry Laboratories, Princeton University, Princeton, New Jersey 08544. *Received June 17, 1983.* This work was supported, in part, by Department of Energy Grant AC02-76ER03120 and National Institutes of Health Grant EY02679.

[1] Abbreviations: L_α, lamellar; H_{II}, inverse hexagonal; C_{II}, inverse cubic; PE, phosphatidylethanolamine; PC, phosphatidylcholine; CL, cardiolipin; PS, phosphatidylserine; Ca^{2+}, calcium ion; T_c, gel to liquid-crystalline transition temperature.

0006-2960/84/0423-1093$01.50/0

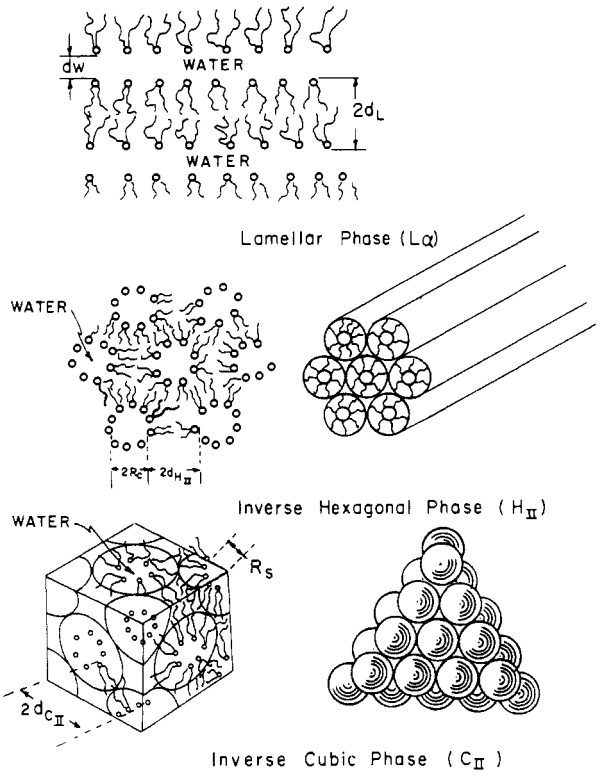

FIGURE 1: Schematic representation of the three phases considered in the model. The L_α phase is an infinite array of planar sheets of thickness d_W and $2d_L$. The H_{II} phase is an infinite array of tubes stacked hexagonally. The C_{II} phase is a cubic close-packed arrangement of inverted spherical micelles. In both the H_{II} and C_{II} phases, the matrix between the water cylinders and spheres is completely filled with hydrocarbon chains. The lines defining the outer radii in the H_{II} and C_{II} phases are for ease of visualization and do not represent real boundaries to the lipid tails.

1982), and fusion junctions (Verkleij et al., 1980; Cullis & deKruijff, 1979).

Lipids in water represent a particular class of lyotropic liquid crystals (Pershan, 1982; Friberg, 1974). These are multicomponent systems containing amphiphilic molecules together with a polar or nonpolar solvent or both. Concentration of a component is a thermodynamic variable, like temperature, that controls the phase behavior. For example, the sodium caprylate–decanol–water system exhibits micellar, inverse micellar, lamellar, hexagonal, and inverse hexagonal phases as the relative concentrations of all three substances are varied at 20 °C (Danielsson, 1976). Winsor (1970) attempted to explain this type of phase diagram in terms of the tendency for the amphiphilic surfaces within the mixture to curve toward the polar regions or toward the nonpolar regions. Although not a quantitative treatment, Winsor's "R" theory describes the consistent decrease in the mean curvature of the shapes defined by the amphiphilic surfaces as lipid concentration is increased. In this paper, we describe a quantitative treatment that can be generalized to other lyotropic systems.

Theory

Description of the Model. We consider a model in which the lipid free energy is dominated by four terms that can be grouped into two categories. The first is determined from the *average local* properties of the lipid–water interface of a given phase (e.g., area per polar group, mean curvature of the interfacial surface, hydrocarbon chain disorder, hydration of polar heads, etc.). This energy will be calculated as if all neighboring lipid–water interfaces are an infinite distance away, as in a calculation of the L_β to L_α chain-melting transition of an isolated membrane (Nagle, 1973; Marčelja, 1974). It will be shown that the only concentration-dependent variable necessary to compute the local free-energy change is the mean curvature of the lipid–water interface. The mean curvature, in turn, can be generated from the dimensions of each lattice. The second set of free energies comes from *global* considerations taking into account all the relevant geometries of the lattice involved. These include electrostatic terms that depend on the boundary conditions at the lipid–water interfaces, hydration effects that are important over short water spaces, and considerations of packing the acyl chains into critical regions of nonlamellar lattices.

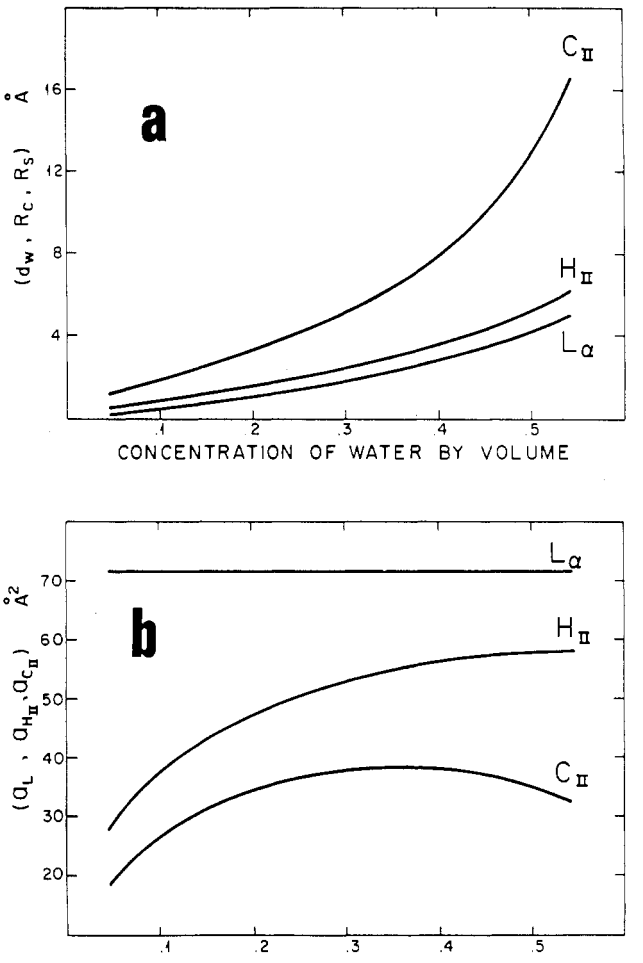

FIGURE 2: Dimensions of the three phases as calculated from the water concentration by using the equations in Table I. (A) Water spacings (L_α, d_W; H_{II}, R_C; C_{II}, R_S) as a function of water concentration. (B) Area per polar group at the lipid–water interface as a function of water concentration.

Three lattices are considered: a lamellar array of bilayers (L_α), a hexagonally packed array of inverted lipid tubes (H_{II}), and a cubic close-packed array of inverted spherical lipid micelles (C_{II}) (see Figure 1). Additionally, it shall be assumed that (i) the temperature is fixed, (ii) water and lipid are incompressible, and (iii) the thickness of a lipid layer (d_L, $d_{H_{II}}$, and $d_{C_{II}}$ in Figure 1) is constant. Assumptions ii and iii are introduced for computational convenience: if the concentration and one of the lattice dimensions are specified, then all of the dimensions of the lattice can be determined through the concentration. These relationships, and the dimensional terminology, are defined in Figure 1 and Table I. The concentration-dependent dimensions are plotted in Figure 2.

The assumptions of incompressibility and constant thickness of the lipid are reasonable approximations to what is observed experimentally. For instance, the lipid volume changes by only

Table I: Calculating Dimensions of the Phases

Definitions (see Figure 1)

C = concentration of water by volume
V_L = incompressible volume per lipid = 1500 Å^3 [a]
d_L = lipid layer thickness in the lamellar phase = 21 Å[a]
$d_{H_{II}}$ = lipid layer thickness in the H_{II} phase = 18 Å[a]
$d_{C_{II}}$ = lipid layer thickness in the cubic phase = 18 Å[a]
a_L = area per head in the lamellar phase
$a_{H_{II}}$ = area per head (at the lipid–water interface) in the H_{II} phase
$a_{C_{II}}$ = area per head (at the lipid–water interface) in the cubic phase
d_W = water spacing between lipid leaflets, lamellar phase
R_C = radius of the water cylinders in the H_{II} phase
R_S = radius of the water spheres in the C_{II} phase

Formulas

$$d_W/(2d_L + d_W) = C \quad (1)$$

$$a_L = V_L/d_L = 71.2 \text{ Å}^2 \quad (2)$$

$$\pi R_C^2/[2\sqrt{3}(R_C + d_{H_{II}})^2] = C \quad (3)$$

$$a_{H_{II}} = 2\pi R_C V_L/[2\sqrt{3}(R_C + d_{H_{II}})^2 - \pi R_C^2] \quad (4)$$

$$(4/3)\pi R_S^3/[\sqrt{32}(R_S + d_{C_{II}})^3] = C \quad (5)$$

$$a_{C_{II}} = 4\pi R_S^2 V_L/[\sqrt{32}(R_S + d_{C_{II}})^3 - (4/3)\pi R_S^3] \quad (6)$$

[a] These constants are chosen to approximate the dimension of natural H_{II}-forming lipid–water systems as determined by X-ray diffraction (Luzzati & Husson, 1962).

3–4% in the L_β to L_α transition (Trauble & Haynes, 1971). Similarly, the lipid thickness in both the lamellar and hexagonal phases changes by only 20–30% while the area per head changes by over 200% and the water width (R_C, d_W) changes by roughly 400% as the concentration of water decreases (Luzzati & Husson, 1962). This is not to say that the contributions of lipid compressibility and thickness are negligible; rather, we assume them to be second-order effects in the determination of the stable lipid phase. Improvements to the model that include a temperature- and concentration-dependent lipid thickness are discussed in the last section.

In the following sections, the total lipid free energy is calculated for each phase by using the lattice dimensions at each concentration (Table I). The stable phase has the lowest free energy at the concentration considered. The concentration where the free energy of the stable phase crosses that of another phase is taken as an estimate of the critical concentration of a mesomorphic phase transition.

Contributions to the Total Free Energy per Lipid Molecule. (*A*) *Local Free Energy.* The local free energy is a collection of different short-range interactions acting on the lipid molecules. Here the contrast between amphiphile systems and simple single-component liquid crystals is strongest. Within the microscopic interface of lipid and water are three distinct regions: (1) the water region, which may be greatly perturbed by the polar groups; (2) the polar group region, which interacts chemically, electrostatically, and sterically with itself and with the water; (3) the hydrocarbon region, which serves to preserve the separation of all three regions through the hydrophobic effect but can also exert pressure on the interface as a result of fluctuations of the flexible hydrocarbon chains.

Several models of the energies of lipid packing exist for different systems (Nagle, 1973; Israelachvili et al., 1977; Jacobs et al., 1975). We are interested in computing the *change* in the local packing energy as the dimensions of each phase change with concentration. In our model, the most significant local change is the decreasing radius of curvature of the lipid–water interface with decreasing water concentration in the hexagonal and cubic phases.

Berde et al. (1980) have developed a theory of the L_β to L_α phase transition in which area per polar group is used as an internal variable. This area is adjusted to minimize the free energy per molecule at each temperature. The lipid free energy is computed from a set of competing terms (Figure 3). An area-dependent cohesive energy ($E = -HA_0/A$) inhibits the chain melting, as does a trans–gauche bond-energy difference (ϵ = 0.6 kcal/mol). Hard-core repulsion between the head groups adds a positive free energy that resists lateral compression of the lipid layer. The free energy associated with this head–head repulsion can be written as a function of $\alpha \equiv (A - A_0)/A_0$, where A is the area per head group and A_0 is the area per molecule occupied by a close-packed two-dimensional array of disk-shaped heads (Figure 3). The free energy of a lipid is then calculated from the partition function of a single molecule summed over all conformational chain states in the presence of these potentials, along with a pressure acting against disordered chain configurations due to hard-core repulsion between neighboring CH_2 groups. Melting occurs with increased temperature because of the larger number of disordered states in the partition function. The hard-core pressure between chains is calculated self-consistently from the average molecular area by using the same two-dimensional hard-disk partition function used to calculate repulsion between the head groups. The equilibrium molecular area and free energy are calculated by minimizing the above free energy over area at each temperature (Figure 3).

We have modified the Berde, Hudson, and Andersen model for our problem by computing the lipid partition function for cylindrical surfaces. The modification changes only the hard-core repulsion between chains, multiplying the effective area change, $\Delta A(i)$, by a factor of $R/[R + l(i)]$. This reflects the decrease in chain pressure allowed by the "splaying out" of the lipid tails. We then calculated the change in equilibrium free energy with the radius of curvature for a 16-carbon disaturated PE at 85 °C according to model S_{III} of Berde et al. The temperature T = 85 °C is used so that this model layer of melted *saturated* lipids is in roughly the same disordered state as natural unsaturated PE membranes at physiological temperatures (Figure 3). The free-energy change $\Delta\mu_{local}$ (R) is approximated by fitting it to a quadratic function of $1/R$ (Figure 3). One obtains

$$\mu_{local} \simeq K_C(1/R - 1/R_0)^2 \quad (7)$$

with $K_C \simeq 2.1$ eV Å^2 and $R_0 \simeq 2.7$ Å. If the calculation is repeated for saturated PC's (using model S_{III} of Berde et al.), the curvature dependence of the equilibrium free energy is not as strong (a 10% decrease in K_C) because the increase in the hard-disk area of the heads diminishes the significance of the chain-pressure term. Of course, a 10% difference in curvature elasticity is not enough to explain the radically different phase behavior of PC vs. PE. Hydration effects (see the following sections) may also contribute importantly to the different phase behavior of PC vs. PE.

In a theory of micelle size distributions of monoacyl soaps, Israelachvili et al. (1975) also postulated an overall head group potential function having the form

$$\mu(a) = (\gamma/a)(a - a_0)^2 + 2a_0 \quad (8)$$

where a = head group area, $\gamma \simeq 0.003$ eV/Å^2 (the surface tension of oil in water), and a_0 = the optimal surface area per head determined by balancing the attractive and repulsive terms but ignoring the hydrocarbon tails. Typical soaps and lipids like PC may have a_0 = 70 Å^2 where PE is probably

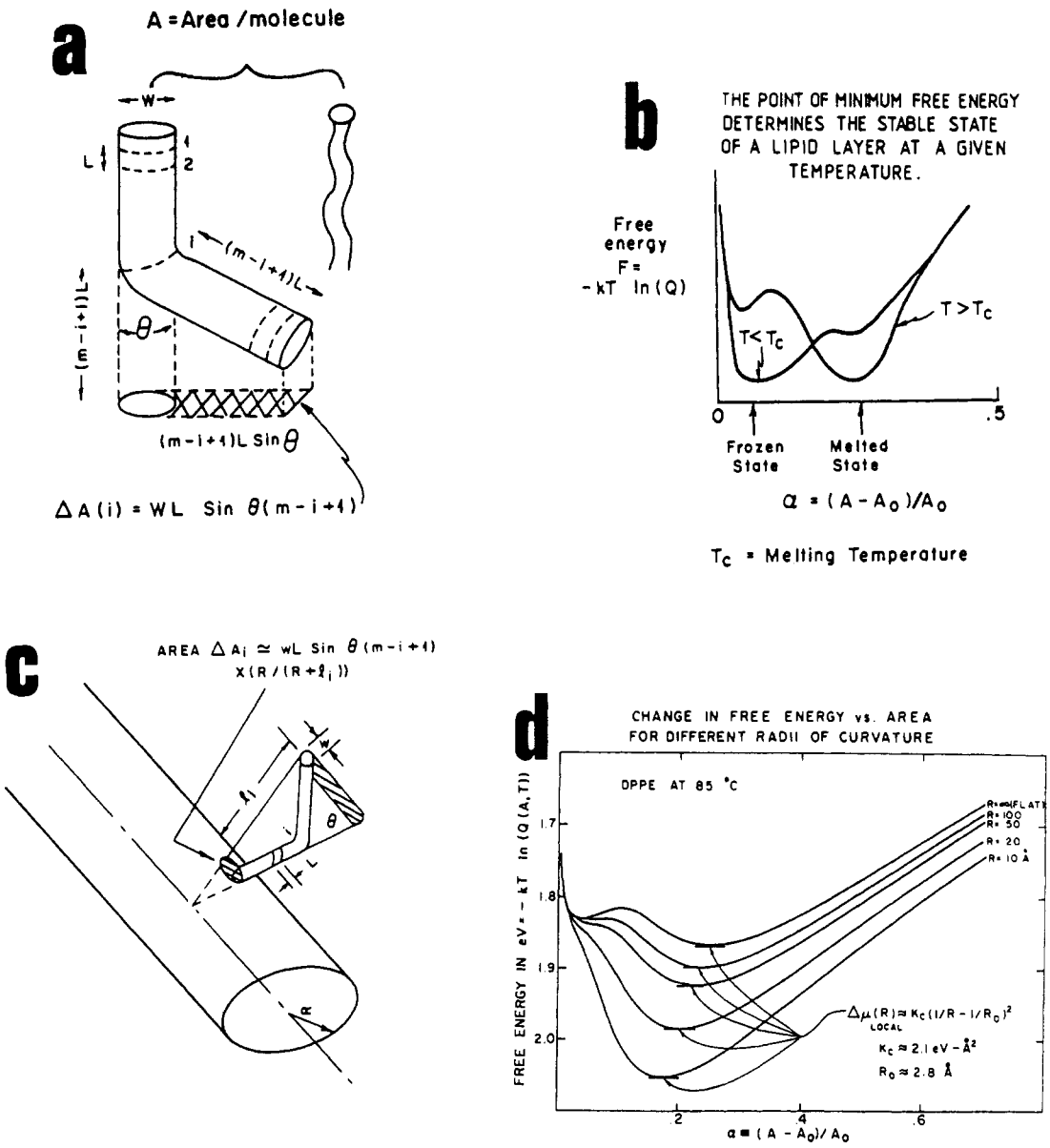

FIGURE 3: Hard-disk model of the chain-melting transition in flat lipid layers due to Berde et al. (1980). (a) Schematic of the representation of an arbitrary state of a lipid molecule labeled by the position of the first gauche kink (i) and the area per polar group (A). The partition function, $Q(A,T)$, contains a cohesive term, $\exp[(A_0/A)H_{sub}(2n + \delta)]$, a hard-disk partition function for the heads, $\alpha^2 A_0 \exp(0.06 - 0.1\alpha + 0.035\alpha^2 + ...)$, and a partition function for the chains, $2\sum_i \exp[[\epsilon(\text{no. of gauche kinks}) + P(A)A(i)]/(kT)]$. Here, A_0 = close-packed area per head group, α = reduced area = $(A - A_0)/A_0$, n = number of CH_2 groups per chain, ϵ = trans/gauche energy difference = 0.6 kcal/mol, H_{sub} = 1.84 kcal/mol, and kT is thermal energy at temperature T. γ and δ are dimensionless parameters adjusted to fit T_c for various PE's; $\gamma = 0.05$ and $\delta = -5.32$. $P(A)$ is a pressure acting against chain disorder calculated from the hard-disk partition function of the heads: $P(A) = kT/[A(2/\alpha + 1.9 + 0.67\alpha + ...)]$. (b) Free energy per lipid of a flat lipid layer as a function of molecular area for temperatures above and below T_c. (c) Modification of the Berde et al. model to include cylindrical geometries. The partition function is changed in only the hard-core chain-pressure term, scaling down the area change by a geometric factor. (d) As the radius of curvature decreases at constant temperature, the chains become more melted, and the equilibrium energy decreases. The energy decrease can be parametrized as a quadratic function of $1/R$.

smaller (a_0 = 40 Å) (Israelachvili et al., 1974) due to its smaller size and greater capacity to hydrogen bond. Israelachvili et al. then assumed the hydrocarbon region to be an incompressible fluid and combined this with the geometry of spheres to generate the following packing equation:

$$N = \text{no. of lipids in a micelle} = \frac{4\pi R^3}{3V_L} = \frac{4\pi R^2}{a_N} \quad (9)$$

where a_N = area per head of an N micelle and V_L = incompressible lipid volume.

From eq 8 and 9 a chemical potential $\mu_N = \mu_R$ can be generated as a function of the size of the micelle. The Israelachvili model may be extended to monomolecular lipid layers, considered in isolation, of an arbitrary curvature $1/R$ and thickness d_L. In this case, one obtains a packing equation (Figure 4):

$$N = A/a_R = (Ad_L/V_L)[1 + d_L/(2R)] \quad (10)$$

where $a_R \equiv$ area per head at curvature $1/R$. Equations 8 and 10 yield a free energy:

$$\mu_R \simeq \frac{\gamma d_L V_L}{4}\left[\frac{1}{R} - \left(\frac{1}{d_L} - a_0{}^2\frac{d_L}{V_L{}^2}\right)\right]^2 + \text{constants} = K_C\left(\frac{1}{R} - \frac{1}{R_0}\right)^2 + \text{constants} \quad (11)$$

Here, $K_C = \gamma d_L V_L/4 = 20$ eV Å^2 and $R_0 \simeq d_L \simeq 18$ Å if $a_0/V_L \ll 1/d_L$. Equation 11 is derived from an expansion of

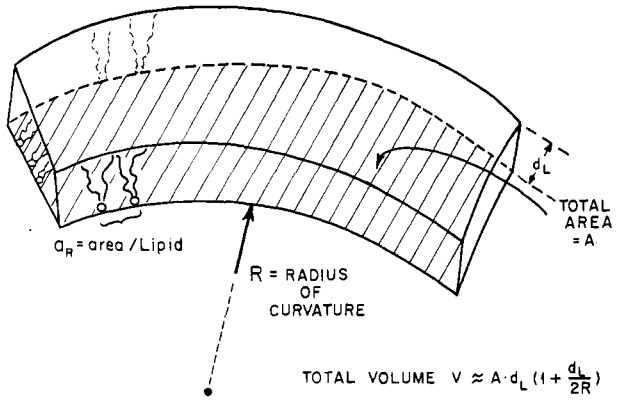

FIGURE 4: Schematic of the packing of lipids in a surface of curvature $1/R$, thickness d_L, and area A at the head group surface to first order in d_L/R. The volume available for packing lipids is approximately $Ad_L[(1 + d_L)/(2R)]$.

N and μ_R in powers of d_L/R; therefore, it should be considered only for $d_L \ll R$. In this region, formulae 7 and 11 are similar in magnitude, and we have assumed that the lipid thickness d_L remains constant with R. A variable-thickness d_L will contribute to the curvature-dependent packing energy somewhat, but the bulk of the response of an *isolated* monolayer to curvature is contained in eq 11. Equations 7 and 11 may then be interpreted as describing a potential that arises from elastically stressing a lipid monolayer of nonzero intrinsic curvature.

Deuling & Helfrich (1976) have also considered the effects of membrane curvature elasticity but have confined their discussion to *bilayer* curvature. This was used to explain the equilibrium shapes of red blood cells. They arive at a two-dimensional free-energy density, g, of the form

$$g \equiv \text{energy per area} = (1/2)K(c_1 + c_2 - c_0)^2 \quad (12)$$

where $c_0 = 1\ \mu m^{-1}$ and $K \simeq 0.3$ eV. Here, c_1 and c_2 are the principal curvatures of the surface, and c_0 is the equilibrium curvature. In the cylindrical monolayer formalism of this paper, $c_1 + c_2 = c = 1/R$. Equation 12 involves twice as many molecules per area (because of the bilayer) and a fundamentally different equilibrium radius of curvature, c_0. The c_0 used by Deuling and Helfrich is the net equilibrium curvature of two opposing monolayers. For an isolated bilayer composed of two identical monolayers, $c_0 = 0$; i.e., the monolayer curvatures cancel. In biological bilayers, c need not be zero because these bilayers usually have monolayers of different compositions and curvatures. Nonetheless, this is why c_0 can be as small as the $1\text{-}\mu m^{-1}$ value postulated by Deuling and Helfrich. Note that the derived monolayer elastic constant

$$K_C = (1/4)a_0K = 4 \text{ eV Å}^2$$

is of the same magnitude as that in eq 7.

We summarize this section with Figure 5A, which shows the variation of the local lipid free energy, μ_{local}, vs. concentration for the lamellar, hexagonal, and cubic phases using the curvature elasticity equation (eq 7). The constant local free energy in the lamellar phase is due to its constant curvature. The curvature of a spherical surface is $2/R$.

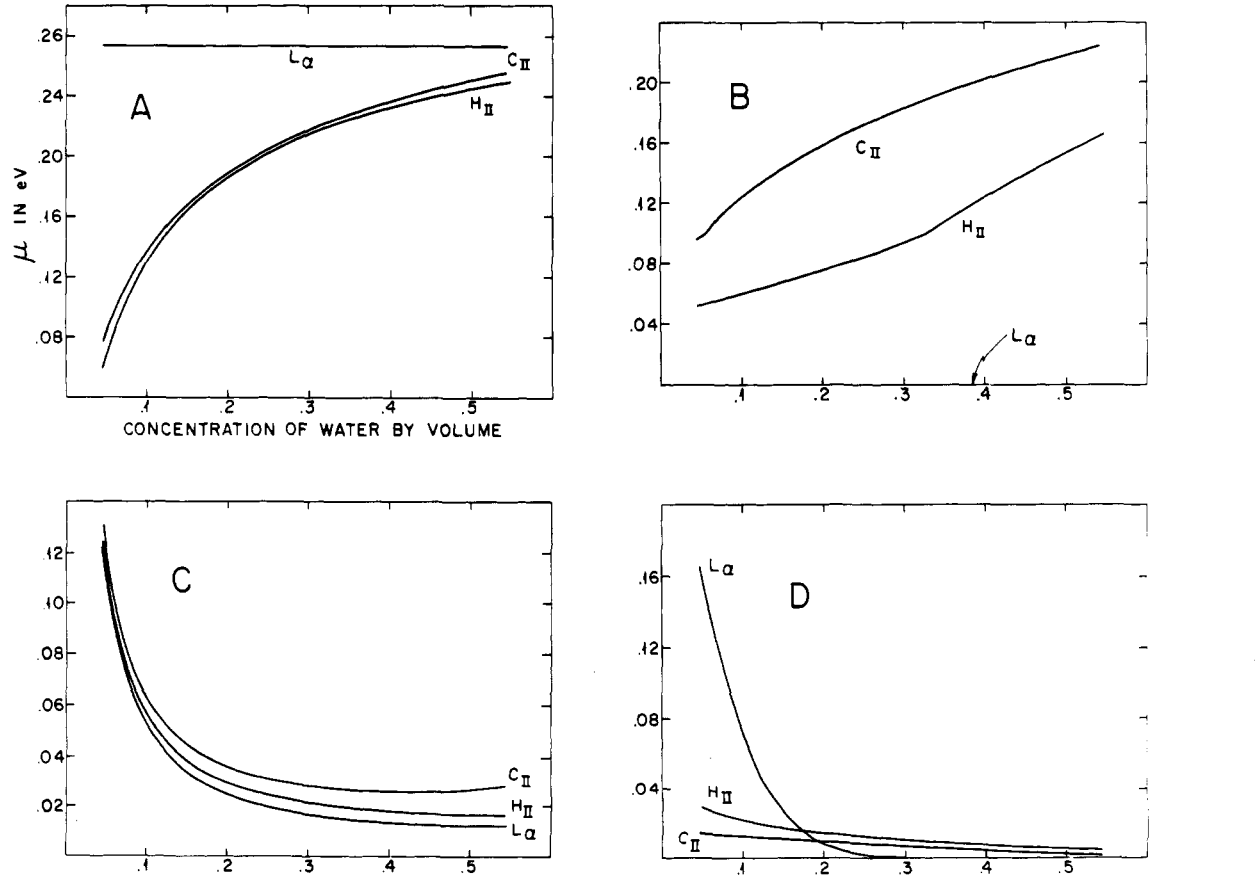

FIGURE 5: The four concentration-dependent free energies that control the phase behavior of a lipid–water system. (A) Local curvature elasticity free energy vs. water concentration from eq 7 and the dimension equations in Table I. (B) Chain-packing free energy using a linear chain stretch energy. The lamellar phase has uniform chain packing, thus zero packing energy. The bends in the curves for the H_{II} and C_{II} phases indicate the onset of vacuum "holes" and an additional surface tension energy. (C) Electrostatic free energy using the solutions to eq 14 and assuming 20% of the lipids are charged (PS). (D) Hydration free energy for each phase using the solutions to eq 15. The necessary physical constants here are (Lis et al., 1982) $[\epsilon/(2\chi)]P_S^2 = 0.015$ eV/Å and $\zeta_{HYD} = 2.5$ Å.

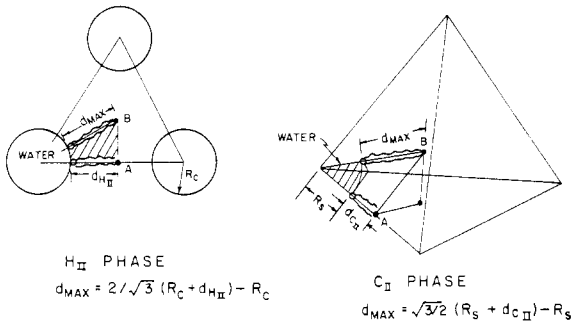

FIGURE 6: Schematic showing the extra length the lipid tails must stretch in order to completely fill the hydrocarbon region between the water cylinders or spheres. The distance from the lipid–water interface to point B, d_{max}, represents the largest distance any lipid must extend.

Table II: Dimensions of the Hexagonal Phase of a Human Brain Lipid Extract at $T = 37$ °C As Determined by X-ray Diffraction (Luzzati & Husson, 1962)[a]

concn of lipid (%)	R_C (Å)	$d_{H_{II}}$ (Å)	d_{max} (Å) $[=(2/3^{1/2})(R_C - d_{H_{II}}) - R_C]$
78	17.6	18.8	24.4
82	14.1	17.5	22.3
85	12.0	17.5	22.0
86	10.9	17.4	21.7
87	10.4	17.1	21.2
89	9.8	17.3	21.5
91	8.1	17.6	21.6
92	7.3	17.9	21.8
95	5.7	18.6	22.3
96	4.7	19.5	23.1
97	4.4	19.6	23.3

[a] For $T = 22$ °C and concentrations greater than 80% the phase is lamellar with a maximum thickness $d_L = 24$ Å. This is roughly the maximum value of d_{max} (24.4 Å) in the H_{II} phase.

(B) Global or Lattice-Specific Contributions to the Free Energy. (1) Chain Packing in Interstitial Spaces. In the hexagonal and cubic phases, there is a systematic variation in the distance over which hydrocarbon chains must stretch in order that the matrix between hydrophilic surfaces be completely filled. For example, in Figure 6, it is seen that tails that extend to point A need not stretch as far as those reaching to point B. One can imagine a lattice for which the maximum tail length, l_C, is such that $d_{H_{II}} < l_C < d_{max}$ (see Figure 6). In this case, vacuum holes will form about point B. We know of no experimental evidence for such holes and, therefore, assume that the energetic cost of forming such holes is high. Supporting evidence for this may be found in the experimentally determined dimensions of lamellar and hexagonal phases, as shown in Table II.

A functional form describing the tail-stretching energy may be derived from the postulate that the free energy of a tail varies linearly as it is stretched from $d_{H_{II}}$ to l_C. The linear form is chosen for simplicity. The energy associated with stretching the chains beyond their "melted" length can be estimated from the free-energy difference between the melted and frozen states obtained from the graphs on Figure 3. The graphs show a difference of as much as 0.2 eV between the local minimum corresponding to the frozen state ($\alpha \cong 0.02$) and the melted state ($\alpha \cong 0.19$). The energy of 0.2 eV is an upper bound on the chain-packing energy since the average lipid is stretched to a length $d_{max}/2$. If d_{max} exceeds l_C, an extra surface tension term is added corresponding to the short-ranged van der Waals energy, E_{VDW}, associated with exposing CH_2 groups to vacuum. The packing free energy is then given by the formulas

$$\mu_{packing} = \Delta E_{stretch}\frac{d_{max} - d_{H_{II}}}{l_C - d_{H_{II}}}$$

for $d_{max} \leq l_C$ and

$$\mu_{packing} = \Delta E_{stretch}\frac{l_C}{d_{max} - d_{H_{II}}} + \Delta E_{VDW}\frac{d_{max} - l_C}{d_{max} - d_{H_{II}}}$$

for $d_{max} > l_C$. Here $\Delta E_{stretch} = 0.1$ eV $= (1/2)$ (the free energy difference between melted and frozen chains at $R = 10$ Å), $\Delta E_{VDW} = 0.25$ eV (from the surface tension of oil in vacuum; Tanford, 1971), and $l_C = 25$ Å. Graphs of $\mu_{packing}$ for all three phases are shown in Figure 5b. Under Discussion, it will be shown how both the curvature-dependent local energy and this lattice-dependent chain-packing energy may be combined.

(2) Electrostatics of Charged Lipids. The addition of phosphatidylserine (PS) to PE is known to inhibit the L_α to H_{II} phase transition (Hope & Cullis, 1979; Cullis & Verkleij, 1979), although PS itself will go into the hexagonal phase if the pH drops below the pK of ionization. This implies that electrostatic inhibition of the H_{II} phase may be a significant term in the total free-energy function. The problem of solving for the free energy of a charged surface in a monovalent ionic medium has been discussed by Verwey & Overbeek (1948), who used the Poisson–Boltzmann equation together with the boundary condition of constant charge density over the lipid–water interface:

$$\nabla^2\psi = (-4\pi q n_0/\epsilon)(\exp[-q\psi/(kT)] - \exp[q\psi/(kT)]) \quad (13)$$

and

$$\mathbf{E}_0 = (-\nabla\psi)_0 = 4\pi\sigma\hat{\mathbf{n}}/\epsilon$$

where ψ = electrostatic potential, n_0 = concentration of monovalent salt, q = electron charge, ϵ = dielectric constant of water, kT = thermal energy at temperature T, $\hat{\mathbf{n}}$ = unit normal to the lipid–water interface, σ = charge density at the interface $= q(\%PS)/\text{area}$, and ψ_0 and $\mathbf{E}_0$ = electric potential and field at the interface.

For pH far from the pK value, we can assume fixed charge density for a given area per polar group so that the energy of the system is (Verwey & Overbeek, 1948)

$$F = \int_{\text{lipid–water interface area}} \psi_0\sigma d^2A$$

where ψ_0 = the potential at the surface. The free energy is then $\mu_{elect} = q\psi_0(\%PS)$. The free energy per lipid molecule depends on the complete boundary conditions of the interface and can be very nonlinear in the limit of large charge densities, so we include this term in the global lattice-dependent free energies. If $q\psi_0 \ll kT$ everywhere, eq 13 can be linearized:

$$\nabla^2\psi = [8\pi q^2 n_0/(\epsilon kT)]\psi = (1/\zeta^2)\psi \quad (14)$$

where $\zeta \simeq 10$ Å for $n_0 = 100$ mM.

The solution to eq 14 in the planar geometry for 10% charged lipids gives $q\psi_0 = 0.03$ eV $\simeq kT$. We will proceed, in any case, to use the linear approximation even up to 60% PS, so as to reproduce the qualitative behavior of the various forces while maintaining a quantitatively tractable set of equations. The full nonlinear Poisson–Boltzmann equation will give different energies, but the order of the phases in terms of the strength of their electrostatic effect and the correct magnitude of energy will be preserved in a linear approximation. The solutions of (14) for planar, cylindrical, and spherical geometries may be shown to be

for the lamellar case

$$\psi(z) = \frac{4\pi\sigma\zeta}{\epsilon} \operatorname{csch} \frac{d_W}{2\zeta} \cosh \frac{z - d_W/2}{\zeta}$$

$$\sigma = \frac{q(\%PS)}{a_L}$$

for the cylindrical case

$$\psi(\rho) = \frac{4\pi\sigma\zeta}{\epsilon} \frac{I_0(\rho/\zeta)}{I_1(R_C/\zeta)}$$

$$\sigma = \frac{q(\%PS)}{a_L}$$

and for the spherical case

$$\psi(r) = \frac{4\pi\sigma\zeta}{\epsilon} \frac{\sinh(r/\zeta)}{(r/\zeta)\left[\frac{\cosh(R_S/\zeta)}{R_S/\zeta} - \frac{\sinh(R_S/\zeta)}{(R_S/\zeta)^2}\right]}$$

$$\sigma = \frac{q(\%PS)}{a_{C_{II}}}$$

where I_0 and I_1 are Bessel functions of the second kind. In all cases, the free energy per lipid molecule $\mu_{elect} = q\psi_0(\%PS)$, where ψ_0 = the potential at the lipid–water interface. The electrostatic free energies, if one assumes 20% PS and uses the constraint equations from section 1, are shown in Figure 5C.

(*3*) *The Hydration Effect.* When hydrated phospholipid bilayers come within 20 Å of each other, an anomalous repulsive force is observed that can become orders of magnitude larger than typical electrostatic forces [see Rand (1981) for an excellent review]. This "hydration force" falls off exponentially with a decay length of less than 3 Å (Lis et al., 1982). The data indicate that water itself is intrinsically involved in the force.

Marčelja (1981) has built upon existing theories of the static and dynamic dielectric constant of ice and proposed a mechanism for this short-ranged repulsion. His model depends on the specific hydration or orientation of water molecules around the polar head groups, most significantly the negatively charged phosphate group. This introduces a surface polarization of the water dielectric even though there are no long-range electric fields present. Away from the dipole surface one would initially expect the polarization density of water to be zero because there are no macroscopic electric fields, but the polarization density cannot instantaneously change from some finite value at the lipid surface to zero without a large energetic cost. Instead, the polarization density should fall to zero quickly in a way that minimizes the following integrated energy density:

$$\mathbf{E} = \int_{\text{water vol}} \mathbf{g}_{HYD}(x)\, d^3x = \int \frac{\epsilon}{2\chi}[|\mathbf{P}(x)|^2 + \zeta_{HYD}^2(\nabla\cdot\mathbf{P})^2]\, d^3x$$

where $\mathbf{P}$ = the three-dimensional polarization density of water, ζ_{HYD} = the correlation length of water = 2.5 Å, ϵ = the dielectric constant of water, and χ = the polarizability of water.

It can be shown that minimizing this energy function is equivalent to solving the *linear* Poisson–Boltzmann equation for an appropriate hydration potential with $-\nabla\psi_{HYD} = \mathbf{P}(\chi)$ and

$$\nabla^2\psi_{HYD} = \frac{1}{\zeta_{HYD}^2}\psi_{HYD} \tag{15}$$

The two-dimensional free-energy density is then

$$E_{HYD/area} = \sigma_{HYD}\psi_S$$

where ψ_S = the hydration potential at the lipid–water interface. The free energy per molecule is

$$\mu_{HYD} = \sigma_{HYD}\psi_S(\text{area/head})$$

We have defined a "hydration charge density" in order to complete the analogy with electrostatics in ionic media. In order to be consistent with the hydration energy of Marčelja, the hydration charge density is

$$\sigma_{HYD} = P_S\left(\frac{\epsilon}{2\chi}\right)$$

where P_S = surface polarization density, and therefore $\mu_{HYD} = P_S\psi_S[\epsilon/(2\chi)](\text{area/head})$. This assumes that the binding of water to the membrane surface does not introduce another *variable* negative free energy besides the energy coming from the three-dimensional positive energy density above. Others have considered an extra binding term (G. Cevc, personal communication), which is equivalent to a constant surface potential assumption in the Poisson–Boltzmann framework (Verwey & Overbeek, 1948). We believe that the hydration of the phospholipids is in a state of saturation in much the same way the charge density of a PS bilayer has leveled off after going well beyond the pK of ionization. The analogy with electrostatics ends, however, when one considers the boundary condition as a function of area per molecule. The measured repulsion between phospholipid bilayers shows a good agreement with an exponential dependence on distance (Lis et al., 1982), at least up to 10-Å separation, even though the area per molecule decreases from 75 to 65 Å^2. In order to be consistent with the linear Poisson–Boltzmann equation (eq 15), P_S must stay constant throughout the 10-Å^2 shrinkage of the surface area per head. In fact, below 10 Å, where the area decreases even more rapidly, the repulsion actually falls below the exponential dependence, let alone the sech $[d_W/(2\zeta_{HYD})]$ dependence predicted by the full solution of eq 15. This indicates that P_S may actually *decrease* as the area per head group decreases. NMR studies using deuterated water and ^{22}Na ions indicate a substantial change in the hydrogen-bonding (Lindblom et al., 1976) arrangement between the polar heads and water as area decreases, especially with PE. PE may tilt its head group dipoles into the plane of the membrane as area shrinks to the L_β area. Complete hydration may be frustrated as the head group matrix becomes tighter. Water molecules may rotate in a way that decreases the effective dipole moment of the "cage" surrounding the phospholipid or actually be removed by substitution with a PE–PE hydrogen bond as the PE head groups tilt toward one another.

The relative magnitudes of the hydration and electrostatic forces between bilayers can be clearly seen (Rand, 1981) when the hydration contribution to the pressure vs. separation curves completely dominates the electrostatic contribution even at 15 Å (five correlation lengths out!). Therefore, an understanding of the correct form for the hydration free energy in all geometries and a knowledge of the correct boundary conditions (P_S vs. area) are crucial in determining whether hydration energies favor or disfavor H_{II} phase formation, let alone determining the correct energy. We will use eq 15 with the boundary polarization P_S taken as a constant equal to the value measured by Lis et al. (1982). With use of the solutions from

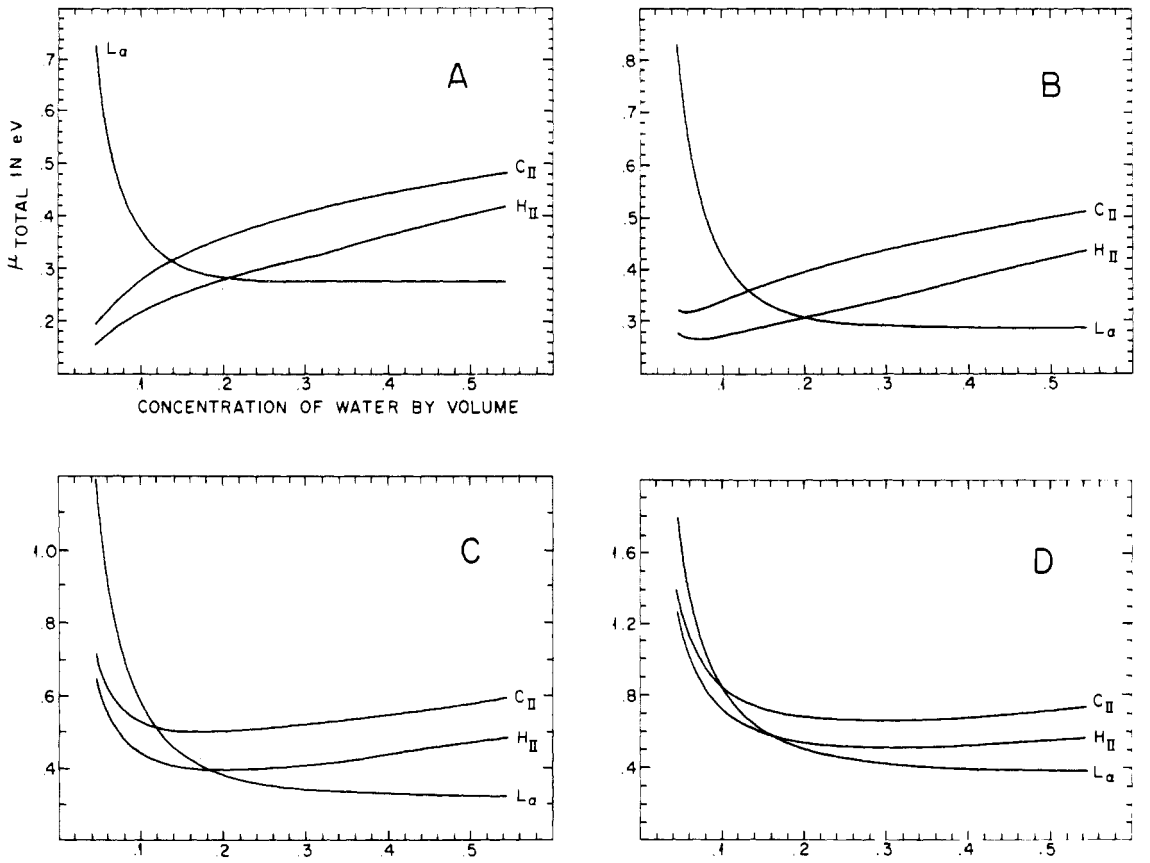

FIGURE 7: (A) Total free energy per lipid molecule for uncharged lipids (PE) vs. concentration of water from the summing of the local curvature elasticity energy, the packing energy, and the hydration energy. (B) Total free energy per lipid molecule for a system of lipids in water, where 80% of the lipids are uncharged (PE) and 20% of the lipids are charged (PS). The total free energy is a sum of the local, packing, hydration, and electrostatic free energies. (C) Total free energy per lipid molecule for a system of 60% PE and 40% PS. (D) Total free energy for 40% PE and 60% PS.

the section on electrostatics, the hydration free energy for each phase is given by

for the lamellar case

$$\mu_{HYD} = \frac{\epsilon}{2\chi}\zeta_{HYD}P_S^2 a_L\left[\coth\frac{d_W}{2\zeta_{HYD}} - 1\right]$$

for the cylindrical case

$$\mu_{HYD} = \frac{\epsilon}{2\chi}\zeta_{HYD}P_S^2 a_{H_{II}}\left[\frac{I_0(R_C/\zeta_{HYD})}{I_1(R_C/\zeta_{HYD})} - 1\right]$$

and for the spherical case

$$\mu_{HYD} = \frac{\epsilon}{2\chi}\zeta_{HYD}P_S^2 a_{C_{II}} \times \left[\frac{\sinh(R_S/\zeta_{HYD})}{\cosh(R_S/\zeta_{HYD}) - \dfrac{\sinh(R_S/\zeta_{HYD})}{R_S/\zeta_{HYD}}} - 1\right]$$

Notice we have subtracted the term

$$\frac{\epsilon}{2\chi}\zeta_{HYD}P_S^2\left(\frac{\text{area}}{\text{head}}\right)$$

from each free energy. This is a self-energy (energy at infinite separation) that really belongs in the local free energy. Since, we assume P_S is constant, this self-energy term is a *cohesive* contribution and may explain why theoretical models like that of Berde et al. (1980) predict a stronger cohesive term than would be expected for simple van der Waals attraction of CH_2 groups. Hydration free energies vs. concentration, from the above equation and the constraint equations of the first section, are shown in Figure 5D.

Results

We now consider different combinations of the four free energies developed in the previous section. First, assume that one is dealing with a system of pure PE and water with no charged lipids present. Figure 7A shows the total free energy per molecule in each of the three phases when the local curvature-dependent free energy, the chain-packing energy, and the hydration free energy are summed. The total free energy is lowest in the lamellar phase for concentrations of water greater than 20%. Below 20% water, the hexagonal (H_{II}) phase has the lowest free energy all the way down to the smallest concentration computed (~4%). The cubic phase (C_{II}) is never predicted to be the stable phase. The crossover at the critical concentration of 20% water arises from the balance of two sets of effects: In one case, the decrease in the local free energy when transforming to the curved H_{II} phase from the flat L_α phase is balanced by the extra chain-packing energy in the H_{II} phase. It is the even larger chain-packing energy that inhibits the C_{II} phase completely. The hydration free energy, by itself, exhibits crossover between the L_α and H_{II} at about 17% water (Figure 5D). There are two competing effects within the hydration free energy that cause this crossover. The solutions to eq 15 in the cylindrical (H_{II}) and sphereical (C_{II}) geometries decay by an inverse power of radius (R_C and R_S) whereas the planar (L_α) hydration free energy decays exponentially with d_W. This results in a larger hydration free energy for the nonlamellar phases at large water

concentrations. As water concentration decreases, the area per polar group decreases in the H_{II} and C_{II} phases, and because of the area independence of the boundary polarization, P_S, this results in a smaller hydration free energy for the nonlamellar phases. The predicted critical concentration of 20% water is within the range of concentrations where the L_α to H_{II} transition is seen in model membrane systems [see Shipley (1973)].

A careful comparison of theory with experiment is difficult because of the occurrence of two-phase coexistence as well as the observation of hysteresis for systems that have not been allowed to come to thermodynamic equilibrium. Two-phase coexistence is, however, thermodynamically allowed in two-component systems such as lipid in water (Callen, 1960). Another possible two-phase coexistence that can be thermodynamically stable is a mesomorphic phase (L_α, H_{II}, or C_{II}) and an excess water phase. Note that the slope of the total free energy vs. water concentration (Figure 7A) is positive in the H_{II} phase. This suggests the possibility for local domains of H_{II} in a lipid–water mixture to push out water into an excess water domain until the *local* concentration of the lipid domain corresponds to a stable state of minimum free energy over concentration for an H_{II} lattice. Figure 7A indicates that the local concentration of an H_{II} phase might decrease well below 10% water until other forces not considered in this model, such as steric factors between the head groups, stabilize the H_{II} domain. This precipitation of H_{II} phase in excess water is observed in the cardiolipin plus Ca^{2+} system and in some synthetic unsaturated PE lipids and may be important in models of defect-mediated bilayer fusion (Cullis & deKruijff, 1979). The slope of the free energy in the H_{II} phase depends critically on the functional form of the hydration free energy, especially the dependence of boundary polarization P_S on area, as well as on the relative magnitude of the hydration term compared to the other two terms.

If one assumes that some fraction of the lipids are charged, then the curves of the total free energy for each phase change somewhat, but the phase behavior over concentration is relatively unchanged. When 20% of the lipids are charged (Figure 7B), the critical concentration for the L_α to H_{II} phase transition is shifted slightly to just below 20% water. At 40% PS (Figure 7C), the critical concentration moves to 18% water. Finally, at 60% PS (Figure 7D) the critical concentration has moved to 16% water, but even at this level of charging the presence of H_{II} phase is still predicted. This implies that the addition of PS to PE–water mixtures does not inhibit the hexagonal phase through simple electrostatics alone. Recall that we have not changed the curvature constants (K_C and R_0) or the hydration term in our model when PS is added. The addition of electrostatics does, however, turn down the slope of the total free energy in the H_{II} and C_{II} phases as water concentration decreases (Figure 7B–D). With enough PS (40–50%), the slope of the H_{II} free energy is negative in the entire region in which the H_{II} phase is stable. This implies the existence of a *stable* lamellar phase for concentrations above 20% water without excess water domains.

Discussion

Our model roughly describes a PE–water system near the L_α to H_{II} critical region with a physically reasonable and consistent set of parameters. It predicts that the C_{II} phase is unlikely in bulk systems. The model exhibits the stabilization of the lamellar phase in excess water upon the addition of charged lipids. However, the complete role of head group conformation in determining the phase behavior remains to be determined.

A number of limitations and approximations should be emphasized for the sake of future improvement. It was assumed that the length of the *lipid* region between two adjacent points on either the lamellar, hexagonal, or cubic lattice was constant over concentration. In fact, the lamellar lipid thickness begins to increase (with the molecular area correspondingly decreasing) as the water concentration decreases below about 20%. There is also no explicit temperature dependence to the parameters used in our model. Most notably, the local curvature free energy depends on two parameters, the curvature elasticity K_C and the equilibrium radius of curvature R_0. These parameters, especially R_0, must certainly be temperature dependent. In the local elastic term, K_C and R_0 were generated by adapting the theory of the gel–liquid crystal states of lipid layers by Berde et al. (1980). In this theory, the equilibrium molecular area (and hence lipid thickness) was calculated at every temperature by minimizing the free energy per molecule. We modified their theory in a very simple way by calculating equilibrium molecular free energy as a function of a *uniform* molecular area on a set of curved surfaces. A more refined modification of their theory to the hexagonal phase would take into account the nonuniform lipid tail conformations throughout the lattice: Where the lipids must stretch to a distance $d_{H_{II}}$ (point A in Figure 6), the area per head group is at a maximum. Where the lipids must stretch to a distance d_{max} (point B in Figure 6), the area per head is at a minimum. If one assumes the area per lipid to vary linearly between these maximum and minimum values as a function of angle around an H_{II} cylinder, then the local molecular free energy should be calculated and averaged over the varying molecular areas around a representative cylinder. An equilibrium average molecular area would then be generated by minimizing the *average* local molecular free energy together with the long-range hydration and electrostatic effects that depend simply on average molecular area. The *average* local molecular energy actually takes into account *both* the local curvature-dependent term and the tail-stretching energy (through the variable molecular area) in a temperature-dependent way. Temperature dependence of the parameters in the hydration and electrostatic terms must also be included. This work is in progress.

A better understanding of the short-ranged hydration force is crucial to developing a numerically accurate and predictive theory of mesomorphic phase transitions in lipid water systems. In fact, the self-energy of hydration of an isolated planar membrane should contribute strongly to the area-dependent free energy per molecule. Thus, hydration effects must be included in theories of the L_β to L_α chain-melting transition, as well as other physical membrane phenomena. A more complete description of the distinct chemical and hydrogen bonding between phospholipid head groups and water and other solutes like Ca^{2+} is needed. A model similar to the present one cannot be developed for cardiolipin or PS in the presence of divalent cations until these specific interactions are understood. Our model lacks specific head group interactions other than those that arise from charge and steric repulsion and the head group specific exponential prefactor in the hydration repulsion.

Experimental tests of the different competing factors in the present model for the L_α to H_{II} phase transitions are necessary. We are investigating the phase behavior of unsaturated PE and water with the addition of a small quantity of a labeled short-chain hydrocarbon. The hydrocarbon should partition into the interstitial spaces at the complementary lattice points (point B in Figure 6) to the water cylinders. This should relieve

the chain-packing stress and allow the H_{II} phase to form at larger water concentrations. The electron-dense marker allows identification of the hydrocarbon partitioning by X-ray diffraction. It is known that unsaturated PE's more readily form the H_{II} phase than saturated lipids. This is probably due to an additional chain pressure toward splay created by a forced kink. A double bond toward the middle of the chain should be more effective in "splaying" out the PE membrane than one placed closer to the ends. We are investigating the phase behavior of a series of synthetic unsaturated PE molecules and water with the double bond moved progressively down the chain.

Experimental data on the effects of hydration and charge on the L_α to H_{II} transition are needed. Experiments similar to the controlled vapor pressure measurements on bilayers (Lis et al., 1982) can be made on H_{II} systems in order to monitor the molecular free energy as water is removed. Finally, a systematic study of the L_α to H_{II} transition as a function of the PS concentration would help clarify the electrostatic contributions.

Acknowledgments

We thank V. A. Parsegian for his valuable advice, P. W. Anderson and G. T. Reynolds for helpful discussions, and B. S. Hudson and C. B. Berde for explanations of their work. Special thanks go to D. S. Hayflick for assistance in preparation of the manuscript.

References

Berde, C. B., Andersen, H. C., & Hudson, B. S. (1980) *Biochemistry 19*, 4279.

Callen, H. B. (1960) *Thermodynamics*, Wiley, New York.

Cullis, P. R., & deKruijff, B. (1979) *Biochim. Biophys. Acta 559*, 399.

Cullis, P. R., & Verkleij, A. J. (1979) *Biochim. Biophys. Acta 552*, 545.

Danielson, I. (1976) *Adv. Chem. Ser. No. 153*, 13.

Deamer, D., Leonard, R., Tardieu, A., & Branton, D. (1970) *Biochim. Biophys. Acta 219*, 47.

deKruijff, B., Verkleij, A. J., Van Echteld, C. J. A., Gerritsen, W. J., Mombers, C., Noordam, P. C., & deGier, J. (1979) *Biochim. Biophys. Acta 555*, 200.

Deuling, H. J., & Helfrich, W. (1976) *Biophys. J. 16*, 861.

Friberg, S., Ed. (1976) *Adv. Chem. Ser. No. 152.*

Hope, M. J., & Cullis, P. R. (1980) *Biochem. Biophys. Res. Commun. 92*, 846.

Israelachvili, J. N., Mitchell, D. J., & Ninham, B. W. (1975) *J. Chem. Soc., Faraday Trans. 2 72*, 152.

Israelachvili, J. N., Mitchell, D. J., & Ninham, B. W. (1977) *Biochim. Biophys. Acta 470*, 185.

Israelachvili, J. N., Marčelja, S., & Horn, R. G. (1980) *Q. Rev. Biophys. 121*, 200.

Jacobs, R. E., Hudson, B. S., & Andersen, H. C. (1975) *Proc. Natl. Acad. Sci. U.S.A. 72*, 3993.

Lindblom, G., Persson, N., & Arvidson, G. (1976) *Adv. Chem. Ser. No. 152*, 121.

Lis, L. J., McAlister, M., Fuller, N., Rand, R. P., & Parsegian, V. A. (1982) *Biophys. J. 37*, 657.

Luzzati, V. (1968) in *Biological Membranes* (Chapman, D., Ed.) Vol. 1, Academic Press, New York.

Luzzati, V., & Husson, F. (1962) *J. Cell Biol. 12*, 207.

Marčelja, S. (1974) *Biochim. Biophys. Acta 367*, 165.

Marčelja, S., Gruen, D. W. R., & Pailthorpe, B. A. (1981) *Chem. Phys. Lett. 82*, 315.

Nagle, J. F. (1973) *J. Chem. Phys. 58*, 252.

Pershan, P. S. (1982) *Phys. Today 35*, 34.

Pinto da Silva, P., & Kachar, B. (1982) *Cell (Cambridge, Mass.) 28*, 441.

Rand, R. P. (1981) *Annu. Rev. Biophys. Bioeng. 10*, 277.

Reiss-Husson, F. (1967) *J. Mol. Biol. 25*, 363.

Shipley, G. G. (1973) in *Biological Membranes* (Chapman, D., & Wallach, D. F. H., Eds.) Vol. 2, Academic Press, New York.

Tanford, C. (1973) *The Hydrophobic Effect*, Wiley, New York.

Trauble, H., & Haynes, D. (1971) *Chem. Phys. Lipids 7*, 324.

Verkleij, A., Van Echteld, C., Gevitson, W., Cullis, P. R., & deKruijff, B. (1980) *Biochim. Biophys. Acta 600*, 620.

Verwey, E. J. W., & Overbeek, J. Th. G. (1948) *Theory of the Stability of Lyotropic Colloids*, Elsevier, Amsterdam.

Winsor, P. A. (1971) *Mol. Cryst. Liq. Cryst. 12*, 141.